A&A 467, 1147–1155 (2007)
DOI: 10.1051/0004-6361:20065686

Astronomy & Astrophysics

Pre-main sequence spectroscopic binaries suitable for VLTI observations⋆,⋆⋆

E. W. Guenther[1], M. Esposito[1,2], R. Mundt[3], E. Covino[4], J. M. Alcalá[4], F. Cusano[1], and B. Stecklum[1]

[1] Thüringer Landessternwarte Tautenburg, Sternwarte 5, 07778 Tautenburg, Germany
e-mail: guenther@tls-tautenburg.de
[2] Dipartimento di Fisica "E.R. Caianiello", Università di Salerno, via S. Allende, 84081 Baronissi (Salerno), Italy
[3] Max-Planck-Institut für Astronomie, Königstuhl 17, 69117 Heidelberg, Germany
[4] INAF – Osservatorio Astronomico di Capodimonte via Moiariello 16, 80131 Napoli, Italy

Received 24 May 2006 / Accepted 6 February 2007

ABSTRACT

Context. A severe problem for research in star-formation is that the masses of young stars are almost always estimated from evolutionary tracks alone. Since the tracks published by different groups differ, it is often only possible to give a rough estimate of the masses of young stars. It is thus crucial to test and calibrate the tracks. Up to now, only a few tests of the tracks could be carried out. However, it is now possible with the VLTI to set constrains on the tracks by determining the masses of many young binary stars precisely.
Aims. In order to use the VLTI efficiently, a first step is to find suitable targets, which is the purpose of this work. Given the distance of nearby star-forming regions, suitable VLTI targets are binaries with orbital periods between at least 50 days and a few years. Although a number of surveys for detecting spectroscopic binaries have been carried out, most of the binaries found so far have periods that are too short.
Methods. We thus surveyed the Chamaeleon, Corona Australis, Lupus, Sco-Cen, and ρ Ophiuci star-forming regions in order to search for spectroscopic binaries with periods longer than 50 days, which are suitable for the VLTI observations.
Results. As a result of the 8 year campaign, we discovered 8 binaries with orbital periods longer than 50 days. Amongst the newly discovered long-period binaries is CS Cha, which is one of the few classical T Tauri stars with a circumbinary disk. The survey is limited to objects with masses higher than 0.1 to 0.2 $M_{\odot}$ for periods between 1 and 8 years.
Conclusions. We find that the frequency of binaries with orbital periods ≤3000 days is of 20 ± 5%. The frequency of long and short period pre-main sequence spectroscopic binaries is about the same as for stars in the solar neighbourhood. In total 14 young binaries are now known that are suitable for mass determination with the VLTI.

Key words. binaries: spectroscopic – stars: formation – techniques: interferometric – stars: pre-main sequence – techniques: radial velocities

1. Introduction

The most fundamental parameter of a star is its mass, which determines almost everything about its birth, life, and death. The masses of low-mass pre-main sequence (pms) stars are often derived by comparing the location of the star in the Hertzsprung-Russell diagram with theoretically calculated evolutionary models. Unfortunately, the evolutionary models published by various authors differ considerably due to the differences in the input physics, such as the treatment of convection, magnetic fields, chemical abundance of the star, etc. (Palla & Stahler 1992; D'Antona & Mazzitelli 1994; Swenson et al. 1994; Burrows et al. 1997; Forestini 1994; Siess et al. 1997; Baraffe et al. 1998; Palla & Stahler 1999; Tout et al. 1999; Chabrier et al. 2000; D'Antona et al. 2000; Wuchterl & Tscharnuter 2003; Montalbán et al. 2004). Testing and calibrating evolutionary models of pms-stars are thus very important for understanding young stars, the determination of the initial mass function, and for studies of the galactic star formation history in general. The lack of knowledge about which models to choose, is thus a severe problem for the whole field of star-formation. Classical T Tauri stars (henceforth called CTTSs) are young, low-mass, optically visible pms-emission line stars with an accretion disk. Weak-line T Tauri stars (WTTSs) are similar to the classical ones but have much lower accretion rates and less massive disks, if any.

An ideal test of the tracks would be to compare the true masses of CTTSs and WTTSs with the masses derived from the models. This is, for example, possible for eclipsing binary stars. Unfortunately, by now there are only three eclipsing young binaries known after eliminating RX J1608.6-3922 by showing that it is not an eclipsing binary but a spotted single star (Joergens et al. 2001). Casey et al. (1998) derived the masses of the eclipsing binary TY CrA to 3.16±0.02 $M_{\odot}$ and 1.64±0.01 $M_{\odot}$ and compared these values with three sets of models. Evolutionary models do not differ too much in the mass range between 1.5 and 3.0 $M_{\odot}$, and thus the authors find that all three sets of models are reasonably consistent with the observations. Since many pms-stars have masses lower than 1.5 $M_{\odot}$, it is important to also have direct mass determinations in the low-mass domain. It is thus

⋆ based on observations obtained at the European Southern Observatory at La Silla, Chile in program 62.I-0418(A); 63.I-0096(A); 64.I-0294(A); 65.I-0012(A); 67.C-0155(A); 68.C-0292(A); 68.C-0561(A); 69.C-0207(A); 70.C-0163(A); 073.C-0355(A); 074.A-9018(A); 075.C-0399(A-F).

⋆⋆ Tables 2, 3, 5, 6, 8, 10, 12–20 are only available in electronic form at http://www.aanda.org

better to focus on stars with masses lower than 1.5 $M_\odot$. Covino et al. (2004) analysed the eclipsing binary RX J 0529.4+0041, which consists of a 1.25 $M_\odot$ primary star, and a 0.91 $M_\odot$ companion star and compared these values with three sets of evolutionary models. They find that the models published by Baraffe et al. (1998) and Swenson et al. (1994) are in reasonable agreement with the observations but the ones published by D'Antona & Mazzitelli (1994) are not. Stassun et al. (2004) analysed the eclipsing binary V1174 Ori, which consists of a 1.01 ± 0.02 $M_\odot$ primary and a 0.731±0.008 $M_\odot$ secondary. They find that models by Montalbán et al. (2004) seem to agree with the observations, but those published by Siess et al. (1997) conflict with them.

By measuring the orbital motion of the molecular gas in the disk, Simon et al. (2000) conclude that models of the pms evolution with lower $T_{\rm eff}$ values are in better agreement with the observations (see, e.g., Baraffe et al. 1998; and Palla & Stahler 1999). Another possibility for measuring masses directly is to combine astrometric data obtained with the HST Fine Guidance Sensors with radial velocity (*RV*) measurements. In this way Steffen et al. (2001) derived masses of 1.5 ± 0.2 $M_\odot$ and 0.81 ± 0.09 $M_\odot$ for the binary system NTT 045251+3016. They find that the Baraffe et al. (1998) models with a mixing-length parameter of $\alpha = 1.0$ are closest to the measured primary mass. The models published by D'Antona & Mazzitelli (1994) are clearly inconsistent with the observations. The first determination of the masses of the components of a young binary star using an interferometer has recently been carried out by Boden et al.(2005). They used the Keck interferometer and determined the masses of the two components of HD 98800 B to 0.70 ± 0.06 $M_\odot$ and 0.58 ± 0.05 $M_\odot$. With an age of 8 to 20 Myr, it is much older than a typical T Tauri star. The object is still young enough to be used for testing the tracks. A reasonable agreement with the models published by Baraffe (1998) could only be achieved by assuming a rather low metallicity of the star.

While all these data allow a very first test of evolutionary models, more mass determinations are definitely needed, especially of stars of lower masses. Shown in Fig. 1 is $\log(L/L_\odot)$ versus $\log(M/M_\odot)$ for all young stars of which the masses have so far been derived. However, we should keep in mind that the position of young stars in the Hertzsprung-Russell diagram depends on the history of the accretion rate. Thus, short-period, eclipsing binaries might not be ideal for testing the tracks, because the components might have had recent mass-exchange. An example where this could have been the case is RX J1603.8-3938. In this system both components have almost identical masses but one is a factor two brighter than the other (Guenther et al. 2001).

In order to determine the masses of many more pms-stars over a large mass range we have carried out a survey for long-period binary stars. For single-line spectroscopic binaries (SB1) only the mass-function $f(m) = \frac{m_2^3 \sin^3 i}{(m_1+m_2)^2}$ can be derived using the *RV*-method. If $f(m)$ is combined with the relative astrometric orbit of the two stars (position angle and relative distance of the stars) and if also its parallax is known, the masses of the two stars can be determined. Using this method, we have derived the masses of the two components of the SB1-system EK Dra (König et al. 2005). This system has, however, an age of about 125 Myr and thus, it is not really young. For double-line spectroscopic binaries (SB2), it is possible to measure $m_1 \sin^3 i$ and $m_2 \sin^3 i$. The individual masses of the stars can then be derived if the *RV*-data is combined with the relative astrometric orbit, or if the system is eclipsing.

Unfortunately, the distance to the nearest star-forming regions is so large that binaries that could be resolved with

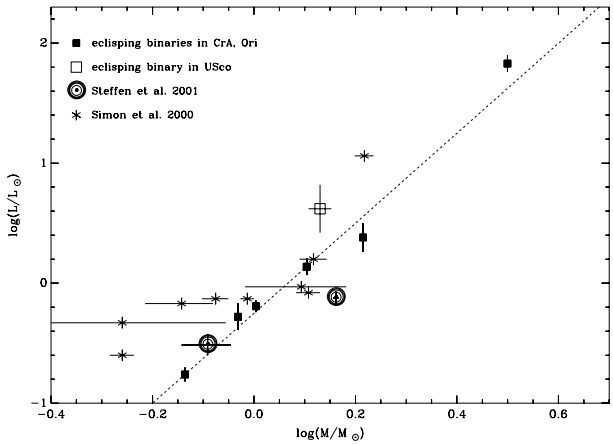

Fig. 1. Current knowledge of empirical mass determination for young stars. The masses of the eclipsing objects in Orion and CrA were taken from Covino et al. (2004), Stassun et al. (2004), and Casey et al. (1998). Alencar et al. (2003) derived the masses of the binary in upper Sco. Using the HST Fine Guidance Sensor, Steffen et al. (2001) determined the masses of NTT 045251+3016 in CrA. Also shown are the masses derived by Simon et al. (2000) by measuring the orbital motion of gas in the disk.

AO-systems on 8 m-class telescopes have orbital periods of many decades, or even centuries. However, the big leap forward in this work is the Very Large Telescope Interferometer, which is now available. The VLTI instrument AMBER (Astronomical Multi BEam combineR) offers the unique opportunity to spatially resolve binaries down to separations of only 4 mas in the *K*-band. Thus, with AMBER it is possible to resolve binaries with separations down to 0.6 AU (corresponding to an orbital period of ∼120 d for systems with $m_1 = m_2 = M_\odot$) for distances ≤150 pc. Because AMBER works in the near infrared, it is possible to detect a young 0.1 $M_\odot$ star next to a young 1.0 $M_\odot$ star due to the achievable brightness-contrast ratio.

To carry out such measurements with AMBER, a sufficient number of pms binaries with suitable separations (i.e. sufficiently long periods) have to be identified first. The aim of this work is thus to identify pms binaries suitable for the VLTI observations. For the survey we selected known pms-stars in southern star-forming regions at a distance ≤150 pc. Stars fainter than 10 mag in the *K*-band, visual pairs with a separation of ≤10 arcsec, and stars with a $v \sin i \geq 50$ km s^{-1} are excluded.

Before we started our survey in 1998, only three pms-spectroscopic binaries with orbital periods longer than 50 days located in nearby star-forming regions were known (Mathieu 1994). Four additional spectroscopic binary *candidates* in the Ophiuchus-Scorpius (Oph), Chamaeleon, Lupus, and Corona Australis star-forming regions were identified by Melo et al. (2003). Thus, while quite a number of authors have already surveyed the nearby star-forming regions for spectroscopic binaries, most of the objects found are binaries with a short period which are unsuitable for VLTI observations. The main intention of our survey is a search for long-period binaries, suitable for VLTI-observations, not a comprehensive survey of spectroscopic binaries. In this paper we present the outcome of this extensive survey. The short-period systems, which were also discovered in the course of the survey, will be subject of a forthcoming paper. In Sect. 2, we describe the observations. In Sect. 3, we give a full list of all long period pms-binaries suitable for the VLTI observations together with the *RV*-values and the orbits of the newly discovered binaries. In Sect. 4, we

Table 1. Spectroscopic binaries with periods longer than 50 days.

	This survey/ region	*EW* Hα	*EW* LiI [Å][1]	Spec type [Å]	m_K type	RA [mag]	Dec (2000.0)	Type (2000.0)	Period [days]
HIP50796[2]	no / TWA	0.20[3]		K5/WTTS	7.66 ± 0.03	10 22 18.0	–10 32 15	SB1	570
CS Cha	yes / Cha	–40	0.53 ± 0.01	K4/CTTS	8.20 ± 0.03	11 02 26.3	–77 33 36	SB1	≥2482
HD97131[4]	no / TWA			F2	7.70 ± 0.02	11 10 34.2	–30 27 19	ST3	134
RX J-7539	yes / Cha	fi	0.21 ± 0.06	K2/WTTS	7.93 ± 0.02	12 20 34.4	–75 39 29	SB1	613
MO Lup[5]	yes / Lup	–2.3	0.37 ± 0.02	K7/WTTS	8.64 ± 0.02	15 24 03.5	–32 09 51	ST3	>3000
RX J1534.1-3916	yes / Lup	abs	0.21 ± 0.02	K1/WTTS	8.55 ± 0.02	15 34 07.4	–39 16 18	SB1	>3000
RX J1559.2-3814	yes / Lup	–1.4	0.23/0.14	WTTS	9.34 ± 0.03	15 59 16.1	–38 14 42	SB2	474
GSC 06209-00735	yes / SC	0.3	0.37 ± 0.01	K2/WTTS	8.43 ± 0.02	16 08 14.8	–19 08 33	SB1	2045
NTTS160814-1857[6]	no / SC	0.7		K2/WTTS	7.69 ± 0.02	16 11 09.0	–19 04 45	SB1	145
GSC 06213-00306	yes / SC	fi	0.24/0.18	WTTS	7.43 ± 0.02	16 13 18.5	–22 12 48	SB2	167
Haro 1-14c[7]	no / Oph			K3/WTTS	7.78 ± 0.03	16 31 04.4	–24 04 33	SB2	591
NTTS162819-2423s[6]	no / Oph	em		G8/WTTS	7.44 ± 0.02	16 31 20.0	–24 30 04	SB1	89
BS Indi[8]	yes / Tuc	abs	0.18 ± 0.02	K0/WTTS	6.57 ± 0.02	21 20 59.8	–52 28 40	SB1	1222

[1] em = emission, abs = absorption fi = filled in; [2] triple system Torres et al. (2003); [3] Song et al. (2002); [4] Torres et al. (2003), possibly also a triple system; [5] triple system consisting of a binary with 12 days, and one of with a period >3000 days. (Esposito et al. 2006); [6] Mathieu (1994); [7] Reipurth et al. (2002), Simon & Prato (2004), eccentricity 0.617 ± 0.008, $f(m) = 0.018 \pm 0.001\ M_\odot$; [8] triple system, see Guenther et al. (2005).

discuss the spectroscopic binary candidates, in the last section we discuss the results.

2. The sample

For our survey we selected 122 late-type pms-stars in the Chamaeleon (Cha), Corona Australis (CrA), ρ Ophiuchi (Oph), Lupus (Lup), and Scorpius Centaurus (SC) star-forming regions. We did not include the 12 SBs known at the start of the survey (Mathieu et al. 1994; Melo 2003; Guenther et al. 2001), and also generally did not include visual binaries, unless the separation was ≥10 arcsec. After the first observing run, we removed another 14 stars from the list, because their v sin i turned out to be too high or because these stars are not young. Apart from the known binaries, and stars with very large v sin im, we observed essentially all stars with spectral types between F6 and M3 in these regions. The sample that was finally observed comprises 108 stars, of which 26 are CTTS and 82 WTTS.

Determinations of the distance of the Chamaeleon association give values of 160 ± 15 pc for ChaI, 178 ± 18 pc for ChaII (Whittet et al. 1997), 171 ± 20 pc for ChaI (Wichmann et al. 1998), and 168^{+14}_{-12} pc (Bertout et al. 1999). For the Corona Australis region Knude & Høg (1998) derive a distance of 170 pc, which is different from the ∼130 pc found by other authors (Knacke et al. 1973; Marraco & Rydgren 1981). For the ρ Ophiuchi region, the distance of 160 pc derived by Knude & Høg (1998) agrees with the results obtained by other authors (Whittet 1974; Chini 1981). Quite a number of authors have determined the distance to the Lupus star-forming region: Hughes et al. (1993) find 140 ± 20 pc, Knude & Høg (1998) 100 pc, Nakajima et al. (2000) 150 pc, Sartori et al. (2003) 147 pc, Franco (2002) 150 pc, de Zeeuw et al. (1999) 142 ± 2 pc, and Teixeira et al. (2000) 85 pc, but note that 14 stars in this group have measured parallax-distances, with an average of 138 pc.

The Upper Scorpius OB association has an age of 5−6 Myr (Preibisch & Zinnecker 1999) and thus is slightly older than the other regions that all have ages of 1−3 Myr. The average distance of the Upper Scorpius OB association is 145 ± 2 pc (de Zeeuw et al. 1999). In Table 1 we also give the parameters of the binaries found in the TW Hydra (TWA) and Tucana (Tuc) associations. Both regions are older but also closer (45−60 pc) than the other regions. Since low-mass stars in these regions are still pms, these objects are interesting for VLTI observations. The TW Hydra region has an age of 8−12 Myr, and the Tucana association an age of about 30 Myr (Webb et al. 1999; Torres et al. 2000; Torres et al. 2003; Weinberger et al. 2004).

3. Observations

All stars were observed with the ESO Echelle spectrograph FEROS (Fiber-fed Extended Range Optical Spectrograph). FEROS was operated up to October 2002 (HJD 245 2550) at the ESO 1.5-m-telescope, and was then moved to the MPG/ESO-2.20-m-telescope. The spectra cover the wavelength region between about 3600 Å and 9200 Å with a resolving power of $\lambda/\Delta\lambda = 48\,000$. On the 1.5-m-telescope the entrance aperture of the fibre had a projected diameter of 2.″7 on the sky, while at MPG/ESO 2.2-m-telescope 2.″0. As long as FEROS was at the ESO 1.5-m-telescope, exposure-times were set so that an *S/N*-ratio of about 30 was achieved. The exposure-times were thus between 5 and 45 min. Since the performance of FEROS dramatically improved when FEROS was moved to the MPG/ESO 2.2-m-telescope, the *S/N*-ratio went up to typically 50, although we shortened the exposure times. The standard FEROS data-reduction pipeline was used for bias subtraction, flat-fielding, scattered light removal, Echelle order extraction, and wavelength calibration of the spectra.

When measuring the radial velocity of stars, the question arises as to whether it is better to use several templates of different spectral types, or only one template. We tried out both methods using HR3862 (G0), HR6748 (G5), HR 5777 (K1), HR5568 (K4), and HR6056 (M0.5) as templates. The advantage in using several templates is that the match between the template and the star is better, but the disadvantage is that the absolute *RV*s of the templates have to be known to a high accuracy, if the absolute *RV*s of a stars are of interest. If the absolute *RV*s of the templates are not well known to a high accuracy, the absolute values of the *RV*s of the stars are lost. In our case this would be a disadvantage, because the first step for detecting pms-spectroscopic binaries is to determine their absolute *RV*. A star with an *RV* that differs by more than 2 km s^{-1} from that of the star-forming region is likely to be either not a member of that region or an SB1.

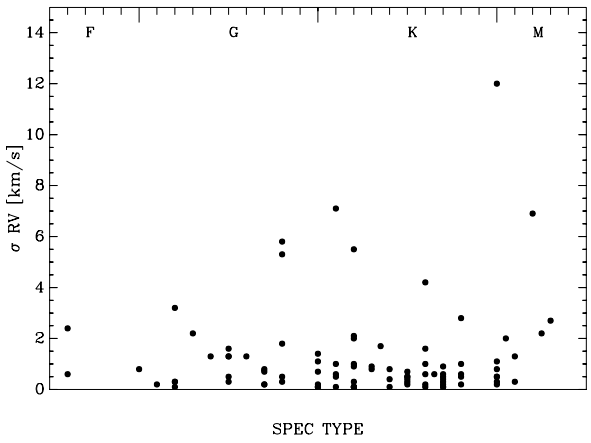

Fig. 2. Scatter of the measurements of all single stars listed in Tables 18−20 versus the spectral type.

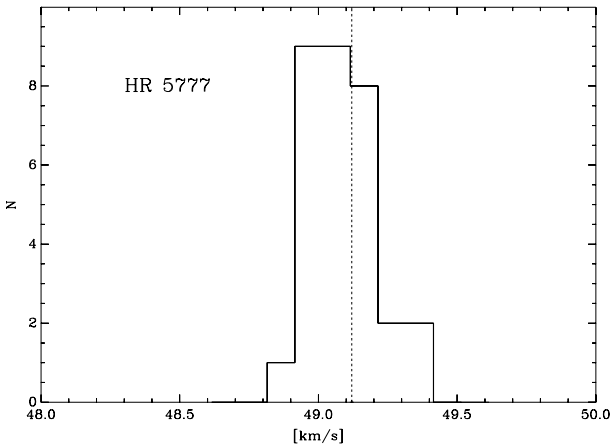

Fig. 3. Histogram of the *RV* measurements obtained for HR 5777. The published *RV* of this star is +49.12±0.06 km s^{-1} (Murdoch 1993), which is shown as a dashed line. The FEROS measurements are consistent with this value. The *FWHM* of a Gaussian-fitted to this the distribution is 0.30 km s^{-1}. The error of the measurements thus is ±0.15 km s^{-1}.

The other alternative is to use just one template. This approach is used in the HARPS search for extra-solar planets of F, G, and K-stars, where an accuracy of typically 1 m s^{-1} is achieved (Lovis et al. 2005). A good choice in our case is the K1-star HR 5777, which is bright (m_v = 4.6), and its absolute *RV* is well-determined (+49.12 ± 0.06 km s^{-1}, Murdoch et al. 1993). If we use just one template, the question is whether the mismatch of the spectral type between the template and the star reduces the accuracy of the *RV*-measurements. If this were the case, the accuracy of the *RV*-measurements of the K-stars would be higher than those of stars with other spectral types. Figure 2 shows the variance of the *RV*-measurements versus the spectral type. Assuming that the scatter is the error of the measurements, we conclude that the error dominated by the v sin i of the stars, and there is no obvious trend with the spectral type. This is possibly because we have only very few M-stars in our survey, where the mismatch with the template really matters. We thus use only HR 5777 as a template. In this way, it is possible to compare the *RV*s of different stars, and it is possible to merge our data with data taken with other instruments.

We split up the spectrum into six wavelength regions which are practically free of stellar emission lines, and virtually free of telluric lines. The wavelength regions are: 4000 to 4850 Å, 4900 to 5850 Å, 5900 to 6500 Å, 6600 to 6860 Å, 7400 to 7500 Å, and 7700 to 8100 Å. For each of the wavelength-band, we obtained the *RV* separately and then averaged these 6 values. The errors in the *RV*-measurements of the T Tauri stars are determined from the variance of the *RV*-values of the individual spectral regions. In many stars, we could use only the first three regions, because the *S/N* ratio of the other regions was too low. In such cases we always used the same regions for the same star. In order to account for any instrumental shift, we measured the position of the telluric spectral lines in the 6860 to 6930 Å region by cross-correlating this part of the stellar spectrum with one taken with the Fourier Transform Spectrometer of the McMath-Pierce telescope at Kitt Peak (Wallace et al. 1998; Brault 1978). We find an instrumental shift of typically 0.5 km s^{-1}, which differs typically by less than 0.1 km s^{-1} from frame to frame.

In order to investigate the accuracy of the *RV*-measurements obtained, we took 31 spectra of HR 5777 spread out over the whole observing campaign. These spectra were reduced in the same way as the spectra of our targets. That is, we used one spectrum of HR 5777 as the template (taken on the March 23, 1999), and cross-correlated this spectrum with all other spectra taken of HR 5777. The absolute *RV* of the template was determined by cross-correlating it with the FTS-spectrum of the sun, which was rebinned to the same resolution as the FEROS spectra (Wallace et al. 1998; Brault 1978). Figure 3 shows a histogram of the *RV*-measurements of HR 5777. The *RV*-values determined for HR 5777 are perfectly consistent with the published *RV* of +49.12 ± 0.06 km s^{-1} (Murdoch et al. 1993). Fitting a Gaussian to this distribution, we derived an *FWHM* of 0.30 km s^{-1}. This implies that the error is ±0.15 km s^{-1}, which agrees well with the error derived from the variance of the *RV*-values, which is ±0.12 km s^{-1}. We thus take ±0.15 km s^{-1} as the intrinsic uncertainty of the measurements. The uncertainty of the *RV*-measurements of the pre-main sequence stars, as determined from the variance of the *RV*-measurements of the individual spectral regions, are usually larger than those of HR 5777, because of the smaller signal-to-noise and the larger v sin i of the stars.

4. Results: long-period spectroscopic binaries

The aim of this survey is to detect young binaries suitable for VLTI-observations, i.e. binaries with orbital periods longer than 50 days located in the nearby star-forming regions. While in our optical observations these systems usually appear as SB1s, many of these can be converted into SB2s, if high-resolution infrared spectra were taken (e.g. Prato et al. 2002). Table 1 gives a short overview of all known long-period binaries in nearby southern star-forming regions found during this study (CS Cha, RX J-7539, MO Lup, RX J1534.1-3916, RX J1559.2-3814, GSC 06209-00735, GSC 06213-00306, BS Indi) and by other authors. In the following, we give details on the individual systems listed in Table 1. In addition to the binaries found in this survey, we also list in Table 1 the long-period spectroscopic binaries published elsewhere (HIP50796, Torres et al. 2003; HD97131, Torres et al. 2003; NTTS160814-1857, Mathieu 1994; Haro 1-14c, Reipurth et al. 2002, Simon & Prato 2004; NTTS162819-2423s, Mathieu 1994). While we cannot completely rule out that the VW Cha and GSC 06793-00569 are binaries, these objects are in any case unsuitable for the VLTI observations, and thus not listed in Table 1.

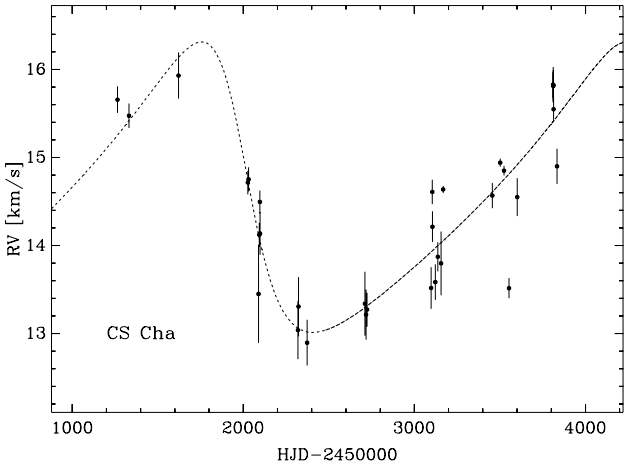

Fig. 4. The *RV*-measurements of the CTTS CS Cha, together with a possible orbital solution with a period of 2482 days.

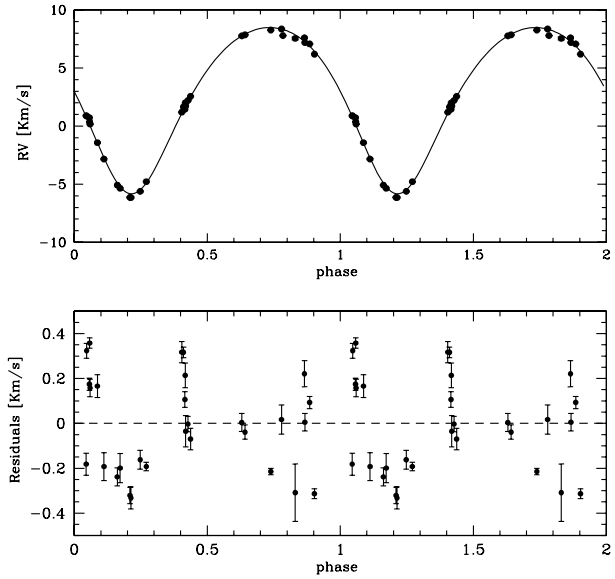

Fig. 5. The phase-folded *RV*-measurements of RX J1220.6-7539. The orbital period is 612.9 ± 0.4 days.

4.1. CS Cha

CS Cha is a CTTS of solar abundance (Padgett 1996). This object was observed by Ghez et al. (1997) by means of speckle-imaging, but no companion was found within 0.″1. However, Takami et al. (2003) already conclude based on a large gap in the inner disk, that this object might actually be a binary. The basic properties of the disk of this star were derived by Henning et al. (1993). We took 32 spectra of this object over a period of 2570 days (Table 2). CS Cha is an SB1-binary system with a very long period. A possible orbit of 2482 days is shown, together with the *RV*-measurements in Fig. 4. The minimum mass of the companion in this case would be only about 0.1 $M_{\odot}$. However, it is still possible that the orbital period is even longer than 2482 days.

4.2. RX J1220.6-7539

RX J1220.6-7539 is a WTTS. In most of our spectra, the Hα line is filled in. In some occasions we observed a small double-line emission profile with an equivalent width of only −0.4 Å. On other occasions, Hα appears in absorption but the equivalent width then is only 0.08 Å. We took 33 spectra of this star over a time-span of 2587 days. The object is an SB1-binary with an orbital period of 613.9 ± 0.4 days and an eccentricity of 0.225 ± 0.005. Figure 5 shows the phase-folded *RV*-measurements. The *RV*-measurements are given in Table 3, and the orbital elements in Table 4.

Table 4. Orbital elements of RX J1220.6-7539.

Element	Value
P	613.9 ± 0.4 d
T_0 [HJD]	2 450 123 ± 3
γ	2.74 ± 0.03 km s^{-1}
K_1	7.15 ± 0.07 km s^{-1}
e	0.225 ± 0.005
ω	171.7 ± 1.9°
$a_1 \sin i$	0.399 ± 0.005 AU
$f(m)$	0.0228 ± 0.0008 $M_{\odot}$

4.3. RX J1534.1-3916

RX J1534.1-3916 is a WTTS, with Hα in absorption. We took 24 spectra of this star over a time-span of 2574 days. The *RV*-values are shown in Table 5 and Fig. 6. The orbital period is certainly much longer than the 2574 days over which we observed the star. Thus we cannot derive an orbit yet. The eccentricity has to be very high (≈0.9). RX J1534.1-3916 nicely illustrates the difficulty in finding long-period spectroscopic binaries with eccentric orbits. If we had not taken the first two spectra, we probably would have classified this object as a single star. According to Hogeveen (1992), only 0.45% of the binaries have $e \geq 0.9$.

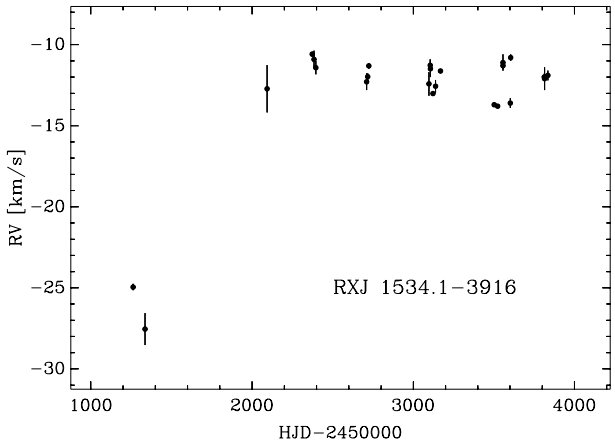

Fig. 6. *RV*-measurements of RX J1534.1-3916, with an orbital period that is apparently longer than 7 years.

4.4. RX J1559.2-3814

RX J1559.2-3814 is a WTTS and an SB2. The average equivalent width of Hα is −1.4 ± 0.2 Å. The equivalent width of the LiI 6708 Å line is 0.23 Å for the primary and 0.14 Å for the secondary component. We find that the ratio of the height of the peak of the cross-correlation function for the two components is 1.9 ± 0.2. Table 6 gives the *RV* measurements obtained for both components, and the orbital elements are listed in the Table 7. A good fit is obtained for a period of 474 days (Fig. 7).

Table 7. Orbital elements RX J1559.2-3814.

Element	Value
P	474.0 ± 1.0 d
T_0 [HJD]	2447834 ± 3
γ	2.0 ± 0.4 km s^{-1}
K_1	13.4 ± 0.2 km s^{-1}
K_2	14.2 ± 0.2 km s^{-1}
e	0.336 ± 0.005
ω_1	336.8 ± 1.9°
ω_2	156.8 ± 1.9°
$a_1 \sin i$	0.549 ± 0.010 AU
$a_2 \sin i$	0.581 ± 0.010 AU
$q = \frac{m_2}{m_1}$	0.945 ± 0.027
$m_1 \sin^3 i$	0.444 ± 0.026 $M_\odot$
$m_2 \sin^3 i$	0.419 ± 0.025 $M_\odot$

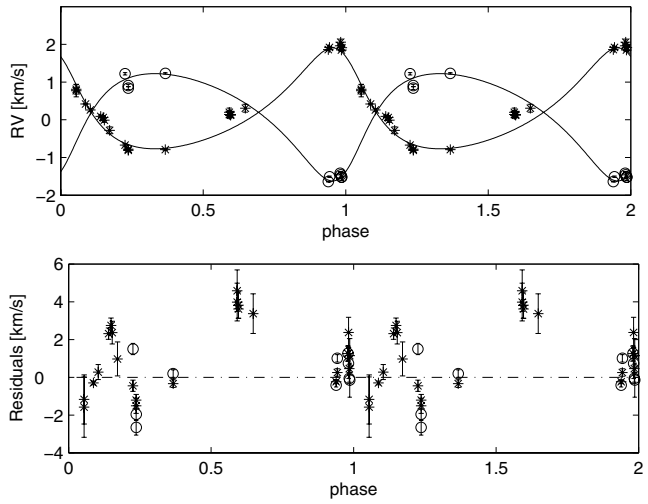

Fig. 7. *RV*-measurements of RX J1559.2-3814. Shown is the orbit of the A and the B component for a period of 474 days.

4.5. GSC 06209-00735

GSC 06209-00735 was first identified as a member of the Upper Sco association based on the spectroscopic and X-ray properties by Preibisch et al. (1998). We confirm the large equivalent width of the LiI 6708 Å line of 0.37 ± 0.01 Å, and found that the object is an SB1. Hα is in absorption, and the equivalent width is 0.3 ± 0.1 Å. In total, we took 26 spectra within 2287 days. We find an orbital period of 2045 ± 16 days, which is only slightly lower than the time over which we observed the star. Figure 8 shows the phase-folded *RV*-measurements together with the orbit. The *RV*-measurements are given in Table 8, and the orbital elements in Table 9.

4.6. GSC 06213-00306

GSC 06213-00306 is another SB2 WTTS. The equivalent widths of the Li I 6708 Å line are 0.241 ± 0.004 Å and 0.18 ± 0.04 Å for the primary and secondary, respectively. The Hα-line is often filled in, and occasionally it appears as an emission line with an equivalent width of −0.1 Å, on other occasions as an absorption line with an equivalent width of 0.1 Å. In total, we took 22 spectra of this binary. We find an orbital solution with a period of 166.9 ± 0.1 days. Thus, GSC 06213-00306 is a long-period, young SB2-binary, the orbital elements for both components have been solved. Given that it has a K-magnitude of 7.43 ± 0.02

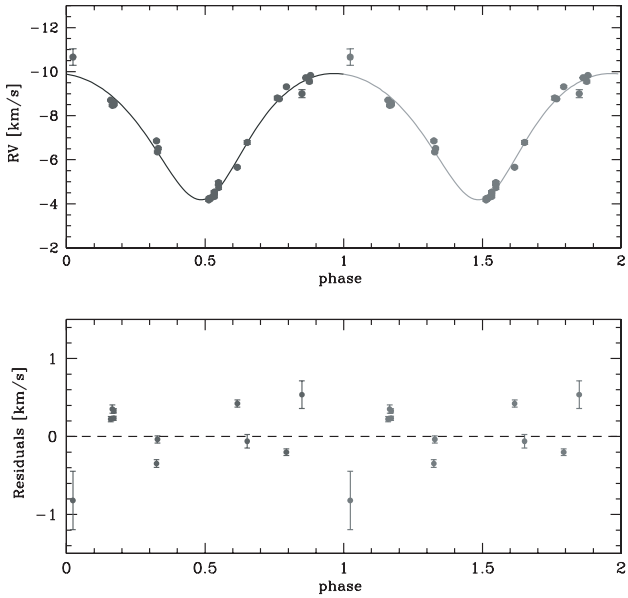

Fig. 8. Phase-folded *RV*-measurements of GSC 06209-00735, with an orbital period of 2045 ± 16 days.

Table 9. Orbital elements of GSC 06209-00735.

Element	Value
P	2045 ± 16 d
T_0 [HJD]	2451022 ± 12
γ	−7.62 ± 0.02 km s^{-1}
K_1	2.87 ± 0.05 km s^{-1}
e	0.20 ± 0.03
ω	8.1 ± 2.3°
$a_1 \sin i$	0.53 ± 0.018 AU
f(m)	0.0049 ± 0.0005 $M_\odot$

Table 11. Orbital elements GSC 06213-00306.

Element	Value
P	166.9 ± 0.1 d
T_0 [HJD]	2452124.2 ± 1.1
γ	−6.76 ± 0.06 km s^{-1}
K_1	15.1 ± 0.1 km s^{-1}
K_2	15.65 ± 0.09 km s^{-1}
e	0.226 ± 0.006
ω_1	161.8 ± 2.2°
ω_2	341.8 ± 2.2°
$a_1 \sin i$	0.226 ± 0.002 AU
$a_2 \sin i$	0.234 ± 0.002 AU
$q = \frac{m_2}{m_1}$	0.97 ± 0.01
$m_1 \sin^3 i$	0.246 ± 0.006 $M_\odot$
$m_2 \sin^3 i$	0.239 ± 0.006 $M_\odot$

it is an ideal VLTI target. The *RV*-measurements are listed in Table 10, the orbit in Table 11. The *RV*-measurements and the orbit are shown in Fig. 9. It is interesting to note that the masses of both components are almost identical.

5. Results: spectroscopic binary candidates

In this section we discuss two objects that were suspected to be spectroscopic binaries with a long period. We argue that in both cases it is unlikely that these are spectroscopic binaries.

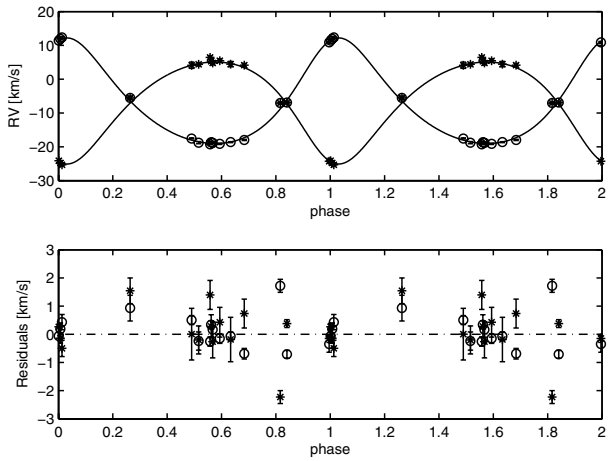

Fig. 9. Phase-folded *RV*-measurements of GSC 06213-00306, together with the residuals. The orbital period is 166.87 ± 0.13 days.

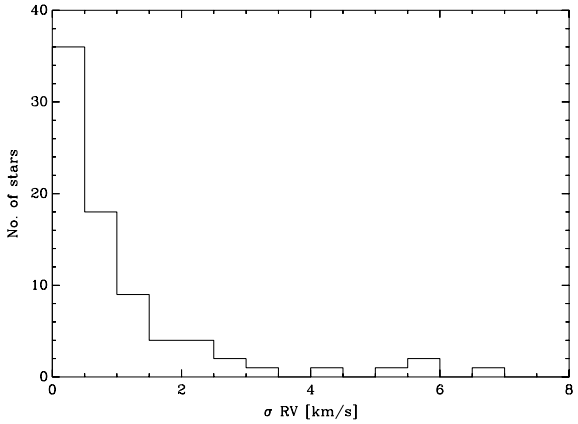

Fig. 10. Histogram of the *RV*-variations observed for the stars listed in Tables 18−20. The amplitude of the *RV*-variations caused are typically less than 3 km s^{-1}.

5.1. VW Cha

VW Cha was already been observed by Melo (2003) with FEROS, who found an occasional doubling of the cross-correlation peak and thus suggested that this object is a spectroscopic binary. Brandner et al. (1996) find that VW Cha is a visual binary with a separation of 0.″72 ± 0.″03. The companion is only 0.25 mag fainter in *J* than the primary. Using *K*-band speckle observations, Ghez et al. (1997) confirm the presence of this companion and determine a separation of 0.″66 ± 0.″03. Surprisingly, Ghez et al. (1997) give a flux-ratio in the *K*-band of 4.5 ± 0.7. In addition to this inner component, Ghez et al. (1997) detected another component with a separation of 17 ± 2″.

As pointed out above, FEROS was operated up to October of 2002 (HJD 245 2550) at the ESO 1.5-m telescope and was then moved to the MPG/ESO-2.20-m telescope. The entrance apertures were 2.″7 and 2.″0 on the ESO 1.5-m telescope, and the MPG/ESO 2.2-m telescope, respectively. Thus, if the fibre is centred on the primary, the secondary would almost be at the edge. The amount of light from the primary and secondary thus would vary depending on the exact placement of the fibre and the seeing. The question thus arises whether the occasional doubling of the spectral-lines is due to this effect, or whether there is really another component. If VW Cha were a spectroscopic binary, its separation would have to be much smaller than 0.″72 ± 0.″03, which implies that we should observe large *RV*-variations.

In order to clarify the situation, we took 16 spectra of this star. The cross-correlation peak is in fact asymmetric. In contrast to our expectation, we find only rather modest variations of the *RV* (Table 12). Additionally, the *RV*-measurements are erratic, and not periodic. While we cannot completely rule out that this is an SB2, it seems more likely that the asymmetric form of the cross-correlation is due to the visual companion moving in and out of the fibre and not due to a spectroscopic companion. This hypothesis would also explain the observed scatter of the *RV*-measurements, because the velocity difference of two stars of one solar-mass are in a circular orbit with a separation of 0.″7 is about 4 km s^{-1}. This object is, in any case, unsuitable for VLTI-observations.

5.2. GSC 06793-00569

GSC 06793-00569 is a WTTS with a weak Hα-emission line of −0.4 Å. We took 19 spectra of this star. Although the cross-correlation occasionally shows a blue asymmetry, and on other occasions a red asymmetry, the *RV*-variations are moderate, and we do not find any significant periodicity (Table 13). We thus interpret the data in the same way as for VW Cha, the star could be a visual binary with such a separation that roughly corresponds to the radius of the fibre.

6. Results: single stars

Unfortunately, not all previous surveys for pms-binaries give a list of the objects that were found to be single. Such a list is, however, very useful, because it avoids duplication of work. In Tables 18−20 we list the average *RV*-values obtained for all single stars together with the variance of the *RV*-values determined for each star. Also given in these tables are the average equivalent widths of Hα and the Li I 6708 Å line, as derived from the spectra. The *K*-band brightness is taken from the 2MASS All-Sky Catalogue of Point Sources (Cutri et al. 2003). The number of spectra taken for each star is given in the last column.

The *RV*-curve of a star with a spot is periodic, where the period corresponds to the rotation period of the star. However, once this spot vanishes and other spots appear at different longitudes, the amplitude and the phase of the *RV*-signal changes. As a result, the periodic signal vanishes, and the power in a periodogram decreases. In contrast to this, the signal of an orbiting companion remains unchaged and thus the power in a periodogram always increases, if more data is added. The difference between the *RV*-signal caused by activity and by an orbiting companion is nicely illustrated for EK Dra, ϵ Eri, and β Gem. EK Dra is an active binary star with an orbital period of 45 years, ϵ Eri is an active star with a planet, and β Gem an oscillating star with a planet (König et al. 2005; Hatzes et al. 2000; Hatzes et al. 2006). For more information on the effects of stellar activity, see also Paulson et al. (2002), and Saar et al. (1998). Variations in the *RV* due to stellar activity have already been observed in T Tauri stars. Because of the activity level of these stars, the effects are even stronger than for older stars. RU Lup, for example, shows *RV*-variations with an amplitude of 2.17 km s^{-1} (Stempels et al. 2007). It is thus not surpising that we observe the same effects in the T Tauri stars that we observed. Nice examples are RX J1415.0-7822 (Table 14, HK Lup, Table 15, GSC 06793-01406 Table 16), and GSC 06793-00994 (Fig. 11), of which we took 13 to 19 spectra each. All of these stars show *RV*-variations with a semi-amplitude of 1 to 3 km s^{-1}, but in none of them could

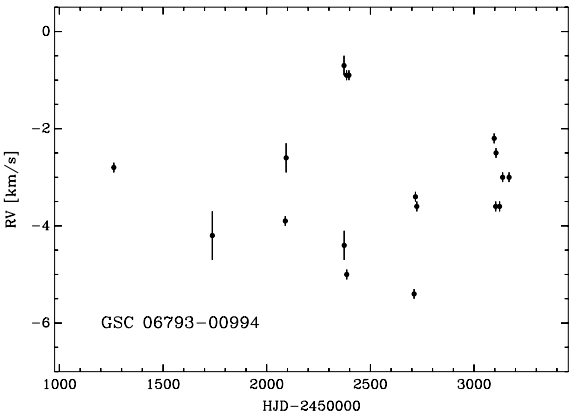

Fig. 11. A typical example of the non-periodic variations of a young star. Shown are the *RV*-values of GSC 06793-00994.

a significant period be detected. Figure 10 shows a histogram of the *RV*-variations observed in single stars.

The survey is limited to companions that cause an *RV*-amplitude of ≥3 km s^{-1}. For example, a system consisting of a 1.0 $M_\odot$ primary and a 0.1 $M_\odot$ secondary would only be detectable, if the period were equal, or shorter, than a year. Similarly, if the companion would have an orbital period of 3000 days, the mass of the companion had to be ≥0.23 $M_\odot$ in order to be detectable. The survey thus is incomplete for long-period companions with masses ≤0.2 $M_\odot$.

We took 13 to 21 spectra of all those stars that show unusually large *RV*-variations, in order to find out whether these are caused by stellar activity or by an orbiting companion. Apart from the objects listed in Table 1, none of them turned out to be a binary. Only in the case of the two rapidly rotating stars GSC 06781-01046 and MN Lup, we cannot fully exclude that they are binaries. One of the spectra of GSC 06781-01046 shows a double-line appearance. This object thus might be an SB2, but more spectra are needed.

7. Discussion and conclusions

The goal of this survey was to compile a list of young long-period binary stars suitable for calibrating the evolutionary tracks by measuring the masses by combining spectroscopic and VLTI data. Although it was not our intention to carry out a statistically complete survey, it does contain some useful informtion on the frequency of young binaries. In his classical review article Mathieu (1994) listed only 3 pms-spectroscopic binaries located in the nearby southern star-forming regions (Chamaeleon, Corona Australis, Lupus, Sco-Cen, ρ Ophiuchi) with orbital periods longer than 50 days and 4 short period systems in these regions. Another short-period binary system (RX J1108.8-7519) was found by Covino et al. (1997). The long-period binaries are NTTS162819-2423S (period 89.1 days, ρ Oph), Wa Oph 1 (=NTTS160814-1857, period 144.7 days, SC), and Haro 1-14c (period 591 days, ρ Oph) (see also Reipurth et al. 2002). NTTS162819-2423S and Haro 1-14c are both members of hierarchical systems. The distance between the spectroscopic binary Haro 1-14c and Haro 1-14 is 12.″9, and NTTS162819-2423S is separated from the spectroscopic binary NTTS162819-2423N by 6.″. In addition to these stars, Melo (2003) identified VW Cha (ChaI), BF Cha (ChaII), CHX 18N (ChaI), and AS 205 (SC) as spectroscopic binaries but did not derive the orbital periods of these objects. However, we do not regard VW Cha as a spectroscopic binary. Another spectroscopic binary found is RX J1603.8-3938 (Guenther et al. 2001). Thus, in all previous surveys, 12 SBs were found: 6 have periods longer than 50 days, and two are triple stars. To these we add 7 long-period SBs and 3 short-period ones. These short-period systems will be discussed in a forthcoming paper (Covino et al. 2007). One of the newly-found long-period systems is a triple star. The newly found triple system is hierarchical. It consists of two components that are separated by 0.″26 ± 0.″03, where one of these components is a binary with an orbital period of possibly 16 days. If we count the triple star as two binaries, because it consists of a long and a short period system, the total number of SBs in these regions is 25. By adding in the previously known binaries, the sample comprises 120 stars in total. Thus, the frequency of SBs is 20 ± 5%. This number can now be compared with the results by Duquennoy & Mayor (1991), who found a frequency of binaries with periods less than 3000 days amongst old G-dwarfs in the solar neighbourhood of 21 ± 4%. The frequency of old and young binaries is thus roughly the same.

Acknowledgements. We are grateful to the user support group of ESO/La Silla. E.C. and J.M.A. acknowledge financial support from INAF and Italian MIUR. This research has made use of the SIMBAD database, operated at CDS, Strasbourg, France. This publication makes use of data products from the Two Micron All Sky Survey, which is a joint project of the University of Massachusetts and the Infrared Processing and Analysis Center/California Institute of Technology, funded by the National Aeronautics and Space Administration and the National Science Foundation. The authors would also like to thank Andrea Mehner for critically reading the text, and the anonymous referee for improving it.

References

Alencar, S. H. P., Melo, C. H. F., Dullemond, C. P., et al. 2003, A&A, 409, 1037
Baraffe, I., Chabrier, G., Allard, F., & Hauschildt, P. H. 1998, A&A, 337, 403
Bertout, C., Robichon, N., & Arenou, F. 1999, A&A, 352, 574
Beuzit, J. L., Hubin, N., Gendron, E., et al. 1994, in Adaptive Optics in Astronomy, ed. M. A. Ealey, & F. Merkle, Proc. SPIE, 2201, 955
Boden, A. F., Sargent, A. I., Akeson, R. L., et al. 2005, ApJ, 635, 442
Brault, J. W. 1978, in Proceedings of JOSO Workshop, ed. G. Godoli, G. Noci, & A. Righini, Arcetri: Osser. Mem. Osserv. Astrofis., 106, 33
Brandner, W., Alcalá, J. M., Kunkel, M., Moneti, A., & Zinnecker, H. 1996, A&A, 307, 121
Burrows, A., Marley, M., Hubbard, W.B., et al. 1997, ApJ, 491, 856
Casey, B. W., Mathieu, R. D., Vaz, L. P. R., Andersen, J., & Suntzeff, N. B. 1998, AJ, 115, 1617
Chabrier, G., & Baraffe, I. 2000, ARA&A, 38, 337
Chini, G. 1981, A&A, 99, 346
Covino, E., Alcala, J. M., Allain, S., et al. 1997, A&A, 328, 187
Covino, E., Frasca, A., Alcalá, J. M., Paladino, R., & Sterzik, M. F. 2004, A&A, 427, 637
Covino, E., et al. in preparation
Cutri, R. M., et al. 2003, VizieR Online Data Catalog: II/246. Originally published in: University of Massachusetts and Infrared Processing and Analysis Center, (IPAC/California Institute of Technology)
D'Antona, F., & Mazzitelli, I. 1994, ApJS, 90, 467
D'Antona, F., Ventura, P., & Mazzitelli, I. 2000, ApJ, 543, L77
de Zeeuw, P. T., Hoogerwerf, R., de Bruijne, J. H. J., Brown, A. G. A., & Blaauw, A. 1999, AJ, 117, 354
Duquennoy, A., & Mayor, M. 1991, A&A, 248, 485
Esposito, M., Covino, E., Alcalá, J. M., Guenther, E. W., & Schisano, E. 2006, MNRAS, submitted
Forestini, M. 1994, A&A, 285, 473
Franco, G. A. P. 2002, MNRAS, 331, 474
Ghez, A. M., Neugebauer, G., & Matthews, K. 1993, AJ, 106, 2005
Ghez, A. M., McCarthy, D. W., Patience, J. L., & Beck, T. L. 1997, ApJ, 481, 378
Guenther, E. W., Torres, G., Batalha, N., et al. 2001, A&A, 366, 965
Guenther, E. W., Covino, E., Alcalá, J. M., Esposito, M., & Mundt, R. 2005, A&A, 433, 629
Hatzes, A. P., Cochran, W. D., McArthur, B., et al. 2000, ApJ, 544, L145
Hatzes, A. P., Cochran, W. D., Endl, M., et al. 2006, A&A, 457, 335
Henning, T., Pfau, W., Zinnecker, H., & Prusti, T. 1993, A&A, 276, 129
Hogeveen, S. J. 1992, Ap&SS, 193, 29

Hughes, J., Hartigan, P., & Clampitt, L. 1993, AJ, 105, 571
Joergens, V., Guenther, E., Neuhäuser, R., Fernández, M., & Vijapurkar, J. 2001, A&A, 373, 966
Knacke, R. F., Strom, K. M., Strom, S. E., Young, E. T., & Kunkel, W. 1973, ApJ, 179, 847
Knude, J., & Høg, E. 1998, A&A, 338, 897
Köhler, R. 2001, AJ, 122, 3325
König, B., Guenther, E. W., Woitas, J., & Hatzes, A. P. 2005, A&A, 435, 215
Lovis, C., Mayor, M., Bouchy, F., et al. 2005, A&A, 437, 1121
Marraco, H. G., & Rydgren, A. E. 1981, AJ, 86, 62
Mathieu, R. D. 1994, ARA&A, 32, 465
Melo, C. H. F. 2003, A&A, 410, 269
Montalbán, J., D'Antona, F., Kupka, F., & Heiter, U. 2004, A&A, 416, 1081
Murdoch, K. A., Hearnshaw, J. B., & Clark, M. 1993, ApJ, 413, 349
Nakajima, Y., Tamura, M., Oasa, Y., & Nakajima, T. 2000, AJ, 119, 873
Padget, D. L. 1996, ApJ, 471, 847
Palla, F., & Stahler, S. W. 1992, ApJ, 392, 667
Palla, F., & Stahler, S. W. 1999, ApJ, 525, 772
Prato, L., Simon, M., Mazeh, T., et al. 2002, ApJ, 569, 863
Quist, C. F., & Lindegren, L. 2000, A&A, 361, 770
Paulson, D. B., Saar, S. H., Cochran, W. D., & Hatzes, A. P. 2002, AJ, 124, 572
Preibisch, T., & Zinnecker, H. 1999, AJ, 117, 2318
Preibisch, T., Guenther, E., Zinnecker, H., et al. 1998, A&A, 333, 619
Reipurth, B., & Zinnecker, H. 1993, A&A, 278, 81
Reipurth, B., Lindgren, H., Mayor, M., Mermilliod, J.-C., & Cramer, N. 2002, AJ, 124, 2813
Saar, S. H., Butler, R. P., & Marcy, G. W. 1998, ApJ, 498, L153
Sartori, M. J., Lepine, J. R. D., & Dias, W. S. 2003, A&A, 404, 913
Siess, L., Forestini, M., & Dougados, C. 1997, A&A, 324, 556
Silverstone, M. D., Meyer, M. R., Mamajek, E. E., et al. 2006, ApJ, 639 [arXiv:astro-ph/0511250]
Simon, M., & Prato, L. 2004, ApJ, 613, L69
Simon, M., Dutrey, A., & Guilloteau, S. 2000, ApJ, 545, 1034
Skrutskie, M. F., Cutri, R. M., Stiening, R., et al. 2006, AJ, 131, 1163
Song, I., Bessell, M. S., & Zuckerman, B. 2002, A&A, 385, 862
Stassun, K. G., Mathieu, R. D., Vaz, L. P. R., Stroud, N., & Vrba, F. J. 2004, ApJS, 151, 357
Steffen, A. T., Mathieu, R. D., Lattanzi, M. G., et al. 2001, AJ, 122, 997
Stempels, H. C., Gahm, G. F., & Petrov, P. P. 2007, A&A, 461, 253
Swenson, F. J., Faulkner, J., Iglesias, C. A., Rogers, F. J., & Alexander, D. R. 1994, ApJ, 422, L79
Takami, M., Bailey, J., & Chrysostomou, A. 2003, A&A, 397, 675
Teixeira, R., Ducourant, C., Sartori, M. J., et al. 2000, A&A, 361, 1143
Torres, C. A. O., da Silva, L., Quast, G. R., de la Reza, R., & Jilinski, E. 2000, AJ, 120, 1410
Torres, G., Guenther, E. W., Marschall, L. A., et al. 2003, AJ, 125, 825
Tout, C. A., Livio, M., & Bonnell, I. A. 1999, MNRAS, 310, 360
Wallace, L., Hinkle, K., & Livingston, W. 1998, An atlas of the spectrum of the solar photosphere from 13 500 to 28 000 cm^{-1} (3570 to 7405 Å) (Tucson: AZ: National Optical Astronomy Observatories)
Webb, R. A., Zuckerman, B., Platais, I., et al. 1999, ApJ, 512, L63
Weinberger, A. J., Becklin, E. E., Zuckerman, B., & Song, I. 2004, AJ, 127, 2246
Whittet, D. C. B. 1974, MNRAS, 168, 371
Whittet, D. C. B., Prusti, T., Franco, G. A. P., et al. 1997, A&A, 327, 1194
Wichmann, R., Bastian, U., Krautter, J., Jankovics, I., & Ruciski, S. M. 1998, MNRAS, 301, L39
Wuchterl, G., & Tscharnuter, W. M. 2003, A&A, 398, 1081

Online Material

Table 2. CS Cha.

HJD	RV [km s^{-1}]
245 1264.54715	15.7 ± 0.2
245 1332.55406	15.5 ± 0.1
245 1621.62514	15.9 ± 0.3
245 2026.54612	14.7 ± 0.1
245 2031.51533	14.8 ± 0.1
245 2089.60062	13.5 ± 0.6
245 2093.54486	14.1 ± 0.1
245 2097.50960	14.5 ± 0.1
245 2098.55118	14.1 ± 0.2
245 2319.67764	13.0 ± 0.3
245 2322.65188	13.3 ± 0.3
245 2373.56573	12.9 ± 0.3
245 2710.51867	13.3 ± 0.4
245 2717.55061	13.2 ± 0.3
245 2723.53930	13.3 ± 0.2
245 3097.51064	13.5 ± 0.2
245 3104.56677	14.6 ± 0.1
245 3105.53213	14.2 ± 0.2
245 3122.55011	13.6 ± 0.2
245 3137.56055	13.7 ± 0.2
245 3155.57941	13.7 ± 0.3
245 3455.56786	14.6 ± 0.1
245 3168.54063	14.6 ± 0.1
245 3501.61418	14.9 ± 0.1
245 3524.53172	14.9 ± 0.1
245 3552.52001	13.5 ± 0.1
245 3601.52246	14.6 ± 0.2
245 3811.53842	15.8 ± 0.2
245 3811.58558	15.8 ± 0.2
245 3811.60357	15.8 ± 0.2
245 3813.78161	15.6 ± 0.2
245 3834.09873	14.9 ± 0.2

Table 3. RX J1220.6-7539.

HJD	RV [km s^{-1}]
245 1262.64298	0.7 ± 0.1
245 1333.65495	−5.4 ± 0.1
245 1621.67014	7.9 ± 0.1
245 1737.48553	7.5 ± 0.1
245 2089.58864	1.2 ± 0.1
245 2093.53472	1.7 ± 0.1
245 2097.55429	2.0 ± 0.1
245 2098.52034	1.7 ± 0.1
245 2319.78210	8.4 ± 0.1
245 2372.63728	7.6 ± 0.1
245 2373.61486	7.2 ± 0.1
245 2384.59905	7.1 ± 0.1
245 2395.67658	6.2 ± 0.1
245 2710.65545	1.4 ± 0.1
245 2717.69773	2.2 ± 0.1
245 2723.66034	2.6 ± 0.1
245 3096.66843	0.9 ± 0.1
245 3097.71156	0.9 ± 0.1
245 3104.70590	0.4 ± 0.1
245 3105.63828	0.2 ± 0.1
245 3122.64088	−1.4 ± 0.1
245 3137.72151	−2.8 ± 0.1
245 3168.57480	−5.1 ± 0.1
245 3455.66760	7.8 ± 0.1
245 3522.60916	8.3 ± 0.1
245 3550.54048	7.8 ± 0.1
245 3811.55386	−6.1 ± 0.1
245 3813.79633	−6.2 ± 0.1
245 3835.16435	−5.6 ± 0.1
245 3849.21861	−4.8 ± 0.1

Table 5. RX J1534.1-3916.

HJD	RV [km s^{-1}]
245 1261.76390	−25.0 ± 0.1
245 1335.77111	−27.5 ± 1.0
245 2093.73652	−12.7 ± 1.5
245 2372.74166	−10.6 ± 0.1
245 2384.71011	−10.9 ± 0.5
245 2395.72062	−11.4 ± 0.4
245 2710.78396	−12.3 ± 0.5
245 2717.78285	−12.0 ± 0.2
245 2723.77086	−11.3 ± 0.2
245 3096.73954	−12.4 ± 0.7
245 3104.77290	−11.3 ± 0.4
245 3105.73478	−11.5 ± 0.5
245 3122.76000	−13.0 ± 0.1
245 3137.77322	−12.6 ± 0.4
245 3168.62275	−11.6 ± 0.1
245 3501.73605	−13.7 ± 0.1
245 3523.74779	−13.8 ± 0.1
245 3556.77084	−11.3 ± 0.2
245 3556.78210	−11.1 ± 0.5
245 3601.55318	−13.6 ± 0.3
245 3603.51374	−10.8 ± 0.2
245 3811.68239	−12.0 ± 0.2
245 3813.84489	−12.1 ± 0.7
245 3835.23052	−11.9 ± 0.3

Table 6. RX J1559.2-3814.

HJD	RV [km s^{-1}] A component	RV [km s^{-1}] B component
245 1264.71496	−6.7 ± 0.3	12.2 ± 0.6
245 1331.71643	−7.9 ± 0.2	12.3 ± 1.1
245 1622.78442	19.6 ± 0.4	−14.2 ± 0.4
245 1623.78926	20.6 ± 0.8	−14.6 ± 0.6
245 1625.71327	19.1 ± 0.9	−15.2 ± 0.7
245 3097.64088	4.2 ± 0.1[1]	
245 3105.69324	2.6 ± 0.4[1]	
245 3122.77331	0.9 ± 0.3[1]	
245 3137.78841	−2.8 ± 0.9	
245 3168.81587	−8.1 ± 0.4	8.4 ± 0.8
245 3168.82963	−7.8 ± 0.3	9.1 ± 1.0
245 3501.75306	18.6 ± 0.1	−16.4 ± 1.1
245 3503.78331	19.2 ± 0.2	−15.1 ± 0.4
245 3523.76173	18.5 ± 0.2	−15.2 ± 1.1
245 3556.79982	7.7 ± 1.6[1]	
245 3556.81105	8.1 ± 1.3[1]	
245 3601.56957	0.6 ± 0.4[1]	
245 3603.53176	−0.1 ± 0.6[1]	
245 3811.70502	2.0 ± 1.1[1]	
245 3811.72015	1.4 ± 1.0[1]	
245 3813.81043	1.4 ± 0.7[1]	
245 3813.82554	1.2 ± 0.5[1]	
245 3838.28599	3.1 ± 1.0[1]	

[1] Just A-component.

Table 8. GSC 06209-00735.

HJD	RV [km s^{-1}]
245 1260.79532	−5.7 ± 0.1
245 1333.79536	−6.7 ± 0.1
245 1622.87285	−9.3 ± 0.1
245 1737.59186	−10.1 ± 0.2
245 2093.77154	−10.4 ± 0.4
245 2395.75208	−8.6 ± 0.1
245 2396.70830	−8.5 ± 0.1
245 2372.81128	−8.7 ± 0.1
245 2384.73607	−8.4 ± 0.1
245 2710.79456	−6.8 ± 0.1
245 2717.79687	−6.4 ± 0.1
245 2723.78469	−6.5 ± 0.1
245 3096.76265	−4.1 ± 0.1
245 3097.75000	−4.2 ± 0.1
245 3104.79092	−4.3 ± 0.1
245 3105.87514	−4.3 ± 0.1
245 3122.78632	−4.4 ± 0.1
245 3137.81404	−4.5 ± 0.1
245 3168.63464	−5.0 ± 0.1
245 3601.59793	−8.8 ± 0.1
245 3616.52275	−8.8 ± 0.1
245 3811.75370	−9.7 ± 0.1
245 3838.36166	−9.5 ± 0.1
245 3847.35257	−9.8 ± 0.1

Table 10. GSC 06213-00306.

HJD	RV [km s^{-1}] A component	RV [km s^{-1}] B component
245 1333.82932	−5.5 ± 0.5[1]	
245 1622.89550	−24.3 ± 0.1	10.9 ± 0.3
245 1623.75952	−24.1 ± 0.1	11.4 ± 0.2
245 1624.73672	−24.8 ± 0.2	11.9 ± 0.2
245 1625.73770	−25.3 ± 0.3	12.4 ± 0.3
245 1737.66113	−18.0 ± 0.2	4.1 ± 0.5
245 2089.46697	−9.0 ± 0.2[1]	
245 2093.50599	−7.0 ± 0.2[1]	
245 2097.59641	−6.9 ± 0.1[1]	
245 2396.72380	4.5 ± 0.8	−18.6 ± 0.2
245 2372.76696	4.1 ± 0.9	−17.5 ± 0.2
245 2384.74816	5.3 ± 0.4	−18.6 ± 0.1
245 2385.71382	4.8 ± 0.6	−18.8 ± 0.3
245 2710.82314	4.4 ± 0.5	−18.8 ± 0.3
245 2717.82525	6.4 ± 0.5	−19.2 ± 0.2
245 2723.81319	5.5 ± 0.5	−19.1 ± 0.2
245 1260.89577	−6.0 ± 0.4[1]	
245 1260.89577	−6.1 ± 0.5[1]	
245 3603.57132	5.7 ± 0.6	−19.7 ± 0.9
245 3811.76438	−2.6 ± 1.0[2]	
245 3813.87632	−2.8 ± 1.0[2]	
245 3838.38271	−7.0 ± 0.4[2]	

[1] both components, unresolved. [2] only the A-component.

Table 12. VW Cha.

HJD	RV [km s^{-1}]
245 1262.57801	14.9 ± 0.5
245 1333.57002	15.4 ± 0.2
245 2031.53243	17.2 ± 0.2
245 2319.70304	19.8 ± 1.0
245 2322.67626	18.6 ± 0.6
245 2372.53625	18.4 ± 1.2
245 2384.53498	15.3 ± 0.4
245 2710.59595	16.3 ± 0.2
245 2717.59503	16.3 ± 0.4
245 2723.58209	22.0 ± 2.4
245 3096.65990	18.7 ± 0.9
245 3104.58111	15.2 ± 0.2
245 3105.55467	17.5 ± 0.1
245 3122.59151	18.4 ± 0.5
245 3137.59880	16.1 ± 0.4
245 3155.64238	14.6 ± 2.6
245 3122.59151	18.5 ± 0.4
245 3522.57695	16.4 ± 0.1
245 3524.54647	18.3 ± 0.4

Table 13. GSC 06793-00569.

HJD	RV [km s^{-1}]
245 1260.90498	−6.5 ± 0.2
245 1333.84131	−4.2 ± 0.3
245 1737.67610	−6.5 ± 0.2
245 2089.47704	−6.8 ± 0.4
245 2093.64727	−4.5 ± 0.4
245 2097.60976	−8.6 ± 0.9
245 2373.71233	−5.7 ± 0.2
245 2385.67462	−5.1 ± 0.1
245 2395.83337	−5.8 ± 0.1
245 2396.81929	−5.7 ± 0.1
245 2710.86108	−7.8 ± 0.1
245 2717.86133	−6.3 ± 0.1
245 2723.82421	−7.0 ± 0.1
245 3097.68383	−5.8 ± 0.1
245 3104.81253	−5.2 ± 0.1
245 3105.78900	−6.2 ± 0.1
245 3122.83664	−5.5 ± 0.1
245 3137.83685	−6.4 ± 0.1
245 3168.70120	−6.9 ± 0.1

Table 14. RX J1415.0-7822.

HJD	RV [km s^{-1}]
245 1261.69317	19.7 ± 0.4
245 1622.67334	18.1 ± 1.3
245 1737.50348	17.1 ± 1.7
245 2019.67697	20.1 ± 0.3
245 2026.69069	19.0 ± 0.6
245 2031.67124	19.1 ± 0.1
245 2098.53621	16.2 ± 1.0
245 2372.67493	21.0 ± 0.2
245 2373.64078	19.3 ± 0.2
245 2384.64679	19.8 ± 0.5
245 2710.69367	19.2 ± 0.3
245 2717.71153	19.0 ± 0.5
245 2723.69779	18.9 ± 0.4
245 3096.86233	18.7 ± 0.2
245 3104.74397	20.3 ± 0.5
245 3105.70977	20.2 ± 0.4
245 3122.73806	18.6 ± 0.5
245 3137.75246	20.5 ± 0.3
245 3168.65138	18.7 ± 0.3

Table 15. HK Lup.

HJD	RV [km s^{-1}]
245 1261.90059	−1.3 ± 0.5
245 1262.69194	−5.0 ± 0.5
245 1622.81043	−5.3 ± 0.7
245 1733.68220	−2.5 ± 0.2
245 2026.83013	−5.2 ± 0.7
245 2031.79988	−5.7 ± 1.2
245 2093.75963	−1.4 ± 0.4
245 2098.59938	−1.9 ± 0.3
245 2395.79978	0.2 ± 0.5
245 2396.77110	4.5 ± 0.2
245 2372.75478	−0.8 ± 0.4
245 2384.72338	−2.3 ± 0.1
245 2385.69702	−0.6 ± 0.1
245 2710.80837	−0.6 ± 0.4
245 2717.81062	−2.3 ± 0.1
245 2723.79847	−0.4 ± 0.1
245 3096.77689	−1.8 ± 0.3
245 3104.80132	−2.3 ± 2.9
245 3105.76881	−8.6 ± 0.4
245 3122.81946	−8.7 ± 0.2
245 3455.75212	1.6 ± 0.8

Table 16. GSC 06793-01406.

HJD	RV [km s^{-1}]
245 1625.80168	−6.9 ± 0.6
245 1737.70415	−7.4 ± 0.6
245 2089.73677	−7.3 ± 0.4
245 2093.78125	−5.8 ± 0.7
245 2384.81131	−5.5 ± 0.1
245 2717.88212	−7.9 ± 0.2
245 2723.87107	−6.8 ± 0.1
245 3096.84966	−5.7 ± 0.3
245 3104.85577	−5.6 ± 0.1
245 3105.83868	−7.1 ± 0.1
245 3122.87716	−7.0 ± 0.2
245 3137.88922	−8.0 ± 0.2
245 3168.74239	−6.2 ± 0.1

Table 17. GSC 06793-00994.

HJD	RV [km s^{-1}]
245 1262.70144	−2.8 ± 0.1
245 1737.69110	−4.2 ± 0.5
245 2089.51975	−3.9 ± 0.1
245 2093.68633	−2.6 ± 0.3
245 2396.80296	−0.9 ± 0.1
245 2372.82468	−0.7 ± 0.2
245 2373.69694	−4.4 ± 0.3
245 2384.79676	−0.9 ± 0.1
245 2385.73404	−5.0 ± 0.1
245 2710.87369	−5.4 ± 0.1
245 2717.83773	−3.4 ± 0.1
245 2723.83505	−3.6 ± 0.1
245 3096.79173	−2.2 ± 0.1
245 3104.83363	−3.6 ± 0.1
245 3105.80278	−2.5 ± 0.1
245 3122.84741	−3.6 ± 0.1
245 3137.84760	−3.0 ± 0.1
245 3168.72226	−3.0 ± 0.1

Table 18. The single stars: Chamaeleon.

	Region	EW Hα[1] [Å]	EW LiI [Å]	Spec type	m_K [mag]	RA (2000.0)	Dec (2000.0)	RV [km s^{-1}]	σ RV [km s^{-1}]	No. of spectra
EG Cha	Cha	−1.1 ± 0.1	0.53 ± 0.01	K7	7.338 ± 0.021	08 36 56.2	–78 56 46	17.4 ± 0.2	0.4	3
EO Cha	Cha	−1.0 ± 0.2	0.53 ± 0.04	M0	8.732 ± 0.021	08 44 31.9	–78 46 31	17.1 ± 0.3	0.5	2
EQ Cha[3]	Cha	−6.5 ± 1.1	0.57 ± 0.04	M3	8.410 ± 0.031	08 47 59.2	–78 54 58	17.9 ± 1.0	2.7	8
RX J0850.1-7554	Cha	abs	0.27 ± 0.01	G5	8.704 ± 0.019	08 50 05.4	–75 54 38	18.1 ± 1.0	1.3	2
RX J0915.5-7609	Cha	−1.1 ± 0.2	0.55 ± 0.03	K6	8.488 ± 0.033	09 15 29.1	–76 08 47	20.3 ± 0.1	0.1	3
RX J0917.2-7744	Cha	abs	0.33 ± 0.06	G2	8.812 ± 0.023	09 17 11.4	–77 44 15	5.7 ± 1.8	3.2	3
HD84075	Cha	abs	0.17 ± 0.01	G2	7.160 ± 0.016	09 36 17.8	–78 20 42	5.2 ± 0.1	0.1	3
HD86356	Cha	fi	0.34 ± 0.05	G8	8.040 ± 0.029	09 51 50.7	–79 01 38	13.2 ± 0.4	0.5	2
HD86588	Cha	abs	0.11 ± 0.01	F6	7.994 ± 0.029	09 53 13.7	–79 33 28	2.4 ± 0.5	2.4	3
RX J1001.1-7913	Cha	−2.5 ± 0.7	0.10 ± 0.01	K8	9.216 ± 0.021	10 01 08.8	–79 13 08	14.4 ± 0.4	0.6	2
RX J1005.3-7749	Cha	−4.2 ± 0.1	0.58 ± 0.01	M1	8.892 ± 0.019	10 05 17.6	–77 49 06	16.3 ± 0.2	0.3	2
SX Cha E[4]	Cha	−20 ± 5	0.65 ± 0.04	M0	8.685 ± 0.024	10 55 59.8	–77 24 40	13.9 ± 0.5	1.1	5
SY Cha	Cha	−13 ± 2	0.56 ± 0.03	M0	8.631 ± 0.019	10 56 30.5	–77 11 39	14.0 ± 0.3	0.5	3
TW Cha	Cha	−28 ± 11	0.41 ± 0.01	K7	8.616 ± 0.021	10 59 01.1	–77 22 41	17.8 ± 0.1	0.1	2
CR Cha (=Sz6)	Cha	−34 ± 2	0.43 ± 0.04	K2	7.310 ± 0.023	10 59 07.0	–77 01 40	16.7 ± 1.1	2.0	3
CT Cha	Cha	−40 ± 21	0.40 ± 0.05	K7	8.661 ± 0.021	11 04 09.1	–76 27 19	15.2 ± 0.3	0.9	13
DI Cha[5]	Cha	−17 ± 1	0.26 ± 0.01	G2	6.217 ± 0.020	11 07 20.7	–77 38 07	14.6 ± 0.2	0.3	2
VW Cha[6]	Cha	−57 ± 11	0.44 ± 0.05	M0.5	6.962 ± 0.026	11 08 01.8	–77 42 29	17.2 ± 0.5	2.0	17
WW Cha[2]	Cha	−57 ± 13	0.3 ± 0.2	K5	6.083 ± 0.053	11 10 00.7	–76 34 59	15.0 ± 2.0	0.5	2
HBC 584	Cha	−77 ± 1	0.3 ± 0.1	K7	9.175 ± 0.024	11 10 49.6	–77 17 52	13.6 ± 0.1	0.2	2
Sz 41[7]	Cha	−2.0 ± 0.9	0.43 ± 0.02	K0	7.999 ± 0.031	11 12 24.5	–76 37 06	14.6 ± 0.3	1.1	18
VZ Cha[2]	Cha	−32 ± 4	0.31 ± 0.01	K6	8.242 ± 0.038	11 09 23.8	–76 23 21	16.3 ± 0.4	0.6	2
CV Cha[2], 5	Cha	−67 ± 16	0.34 ± 0.02	G8	6.845 ± 0.026	11 12 27.7	–76 44 22	16.1 ± 1.2	1.8	2
GSC 07739-02180	SC	−3.9 ± 1.2	0.52 ± 0.01		8.053 ± 0.029	11 21 05.5	–38 45 17	12.1 ± 0.7	1.2	3
RX J1129.2-7546	Cha	fi	0.49 ± 0.02	K3	8.878 ± 0.024	11 29 12.7	–75 46 26	14.6 ± 0.5	0.8	3
RX J1140.3-8321	Cha	−0.3 ± 0.2	0.21 ± 0.01	K2	8.635 ± 0.019	11 40 16.6	–83 21 00	12.7 ± 0.1	0.1	3
RX J1150.4-7704	Cha	−1.3 ± 0.5	0.40 ± 0.06	K2	8.970 ± 0.021	11 50 28.9	–77 04 38	−3.3 ± 1.0	2.1	4
T Cha	Cha	−8.8 ± 9.9	0.41 ± 0.03	G8	6.954 ± 0.018	11 57 13.5	–79 21 32	14.0 ± 1.3	5.3	17
RX J1159.7-7601	Cha	−0.2 ± 0.1	0.46 ± 0.01	K2	8.304 ± 0.027	11 59 42.3	–76 01 26	13.8 ± 0.1	0.1	3
RX J1202.1-7853	Cha	−3.3 ± 0.5	0.56 ± 0.02	K7	8.307 ± 0.023	12 02 03.8	–78 53 01	17.1 ± 0.2	0.3	3
HD106772	Cha	abs	0.21 ± 0.01	G2	6.231 ± 0.031	12 17 26.9	–80 35 06	−12.9 ± 0.2	0.3	2
RX J1219.7-7403	Cha	−4.5 ± 1.6	0.56 ± 0.01	K8	8.858 ± 0.023	12 19 43.8	–74 03 57	13.8 ± 0.1	0.2	2
RX J1220.4-7407	Cha	−2.9 ± 0.6	0.61 ± 0.01	K7	8.367 ± 0.022	12 20 21.9	–74 07 39	12.3 ± 0.4	0.6	2
HD107722	Cha	abs	0.08 ± 0.01	F6	7.135 ± 0.034	12 23 29.0	–77 40 51	13.4 ± 0.4	0.6	2
RX J1233.5-7523	Cha	abs	0.14 ± 0.01	K0	7.756 ± 0.040	12 33 32.0	–75 23 25	15.5 ± 0.1	0.1	2
RX J1239.4-7502	Cha	abs	0.41 ± 0.01	K2	7.777 ± 0.021	12 39 21.3	–75 02 39	13.9 ± 0.2	0.3	2
BC Cha	Cha	−72 ± 18	0.52 ± 0.03		9.354 ± 0.021	13 01 59.0	–77 51 22	14.3 ± 0.2	0.4	2
RX J1325.7-7955	Cha	abs	0.10 ± 0.05	K1	8.932 ± 0.022	13 25 42.8	–79 55 25	−8.4 ± 3.6	7.1	4
CPD-75 902	Cha	abs	0.22 ± 0.01	K0	8.015 ± 0.053	13 49 12.9	–75 49 48	−0.8 ± 0.1	0.2	2
RX J1415.0-7822	Cha	fi	0.26 ± 0.05	G5	9.876 ± 0.023	14 15 01.8	–78 22 12	−3.1 ± 0.3	1.3	18

[1] em = emission, abs = absorption fi = filled in; [2] WW Cha, VZ Cha, CV Cha: also observed by Melo et al. (2003) and found to be single; [3] EQ Cha: difficult object, cc-function asymmetric, unlikely to be binary; [4] SX Cha: visual binary M0 primary and M3 secondary with a separation of 2.″2. (Reipurth & Zinnecker 1993), only eastern component observed; [5] DI Cha (LkHα 332-17): binary with separation of 4.″9 ± 0.″2 (Ghez et al. 1997); [6] VW Cha: triple system, separation of 0.″66 ± 0.″03 and 17.″ ± 2.″ (Ghez et al. 1997); [7] Sz 41: triple system, separation of 1.″5 ± 0.″8 and 12.″4 ± 0.″6 (Ghez et al. 1997).

Table 19. The single stars: Lupus, Scorpius Centaurus.

	Region	EW Hα[1] [Å]	EW LiI [Å]	Spec type	m_K [mag]	RA (2000.0)	Dec (2000.0)	RV [km s^{-1}]	σ RV [km s^{-1}]	No. of spectra
LQ Lup	Lup	−1.5 ± 0.5	0.26 ± 0.03	G8	8.809 ± 0.021	15 08 37.8	–44 23 17	7.6 ± 1.5	5.8	17
LS Lup	Lup	−0.7 ± 0.1	0.47 ± 0.01	K1	9.454 ± 0.021	15 15 52.8	–44 18 16	6.8 ± 0.4	0.5	2
RX J1516.6-4406	Lup	fi	0.54 ± 0.13	K2	9.193 ± 0.019	15 16 36.8	–44 07 19	4.4 ± 1.3	5.5	18
MM Lup	Lup	fi	0.47 ± 0.01		9.260 ± 0.023	15 23 25.7	–40 55 45	4.4 ± 0.1	0.2	3
MN Lup[3]	Lup	−6.1 ± 0.8	0.44 ± 0.05	M2	9.496 ± 0.019	15 23 30.4	–38 21 29	6.6 ± 3.4	6.9	4
MP Lup	Lup	fi[1]	0.36 ± 0.01	K1	8.930 ± 0.019	15 24 32.4	–36 52 02	3.3 ± 0.3	0.6	4
MQ Lup	Lup	−0.5 ± 0.2	0.39 ± 0.03	K2	8.842 ± 0.021	15 25 33.2	–36 13 46	3.6 ± 0.1	0.1	2
MR Lup	Lup	−1.7 ± 0.2	0.47 ± 0.03	K6	8.963 ± 0.019	15 25 36.7	–35 37 32	−1.0 ± 1.9	4.2	5
HIP75836[4]		abs	0.04 ± 0.01	K0	6.760 ± 0.020	15 29 26.9	–28 50 52	−19.5 ± 0.1	0.1	3
MT Lup	Lup	−1.3 ± 0.5	0.48 ± 0.01	K5	9.376 ± 0.024	15 38 02.7	–38 07 22	3.0 ± 0.2	0.3	2
RX J1538.6-3916	Lup	abs	0.39 ± 0.01	K4	8.854 ± 0.023	15 38 38.3	–39 16 54	2.5 ± 0.2	0.4	3
RX J1539.2-4455	Lup	−1.8 ± 0.4	0.17 ± 0.03		9.989 ± 0.021	15 39 12.0	–44 55 29	5.5 ± 0.1	0.1	2
MU Lup	Lup	−0.8 ± 0.1	0.49 ± 0.01	K6	9.187 ± 0.026	15 40 41.2	–37 56 18	2.2 ± 0.1	0.2	2
GSC 06785-00476	SC	abs	0.30 ± 0.01	G7	8.920 ± 0.023	15 41 06.8	–26 56 26	−2.0 ± 0.1	0.2	3
GSC 06781-01046[5]	SC	abs	≤0.2	G5	8.177 ± 0.020	15 42 49.9	–25 36 41	SB2?	–	2
GW Lup[2]	Lup	−52.8 ± 6.8	0.48 ± 0.04	M0	8.630 ± 0.021	15 46 44.7	–34 30 36	−3.5 ± 0.5	0.8	2
HBC 603[6]	Lup	−10.4 ± 2.2	0.58 ± 0.01	M0	8.271 ± 0.026	15 51 47.0	–35 56 43	−2.6 ± 0.1	0.2	3
RX J1555.4-3338	Lup	−0.7 ± 0.5	0.44 ± 0.01	K5	9.353 ± 0.022	15 55 26.3	–33 38 22	0.0 ± 0.1	0.2	3
HD142987	SC	−2.1 ± 0.1	∼0.3	G3	7.614 ± 0.021	15 58 20.6	–18 37 25	6.0 ± 1.5	2.2	2
GSC 06191-00552	SC	−0.6 ± 0.1	0.48 ± 0.01	K3	8.325 ± 0.024	15 58 47.8	–17 57 59	−6.4 ± 0.5	0.9	3
GSC 06195-00768	SC	−0.5 ± 0.2	0.46 ± 0.02	K7	8.372 ± 0.025	15 57 02.4	–19 50 41	−5.1 ± 0.2	0.5	4
HBC 609	Lup	−30 ± 1.0	0.39 ± 0.06	K8	8.608 ± 0.023	15 59 16.5	–41 57 09	0.2 ± 0.7	1.0	2
RY Lup	Lup	−3.2 ± 0.3	0.38 ± 0.01	G0	6.976 ± 0.019	15 59 28.4	–40 21 51	−0.4 ± 0.5	0.8	2
MZ Lup	Lup	abs	0.33 ± 0.02	G8	8.528 ± 0.030	16 01 09.0	–33 20 14	1.8 ± 0.2	0.3	2
GSC 06204-00812	SC	−0.1 ± 0.1	0.47 ± 0.01	K4	8.727 ± 0.025	16 03 02.7	–18 06 04	−4.9 ± 0.1	0.1	2
GSC 06784-01219	SC	−0.1 ± 0.1	0.37 ± 0.01	G7	8.461 ± 0.023	16 05 50.5	–25 33 12	−4.2 ± 0.1	0.2	2
EX Lup[2]	Lup	−24 ± 8	0.36 ± 0.08	M0	8.496 ± 0.021	16 03 05.5	–40 18 25	−0.3 ± 0.1	0.3	3
HBC 613	Lup	−32 ± 2	0.46 ± 0.02	K8	8.724 ± 0.023	16 07 10.0	–39 11 03	−0.5 ± 0.3	0.5	2
NQ Lup	Lup	−1.4 ± 0.1	0.51 ± 0.03	K7	8.714 ± 0.021	16 08 18.3	–38 44 04	0.8 ± 0.1	0.1	2
GSC 06784-00039	SC	fi	0.37 ± 0.01	G7	7.908 ± 0.016	16 08 43.4	–26 02 17	−4.6 ± 0.5	0.7	2
HK Lup[2]	Lup	−22 ± 17	0.54 ± 0.03	K8	8.014 ± 0.021	16 08 22.5	–39 04 46	−2.2 ± 0.8	2.8	21
V1094 Sco	Lup	−8.2 ± 3.3	0.49 ± 0.02	K6	8.658 ± 0.021	16 08 36.2	–39 23 03	0.4 ± 0.3	1.0	9
GSC 06793-00868	SC	−2.8 ± 0.2	0.55 ± 0.01	M1	8.815 ± 0.034	16 11 56.4	–23 04 04	−6.0 ± 0.8	1.3	3
GSC 06793-00797	SC	−0.7 ± 0.2	0.52 ± 0.01	K4	8.455 ± 0.027	16 13 02.8	–22 57 43	−6.5 ± 0.4	0.8	4
GSC 06793-00569[7]	SC	−0.4 ± 0.2	0.47 ± 0.20	K1	8.494 ± 0.019	16 13 29.3	–23 11 06	−6.1 ± 0.2	1.0	19
GSC 06793-00994	SC	−0.3 ± 0.2	0.38 ± 0.01	G4	8.608 ± 0.023	16 14 02.1	–23 01 01	−3.1 ± 0.3	1.3	18
GSC 06801-00186	SC	abs	0.35 ± 0.02	G5	8.686 ± 0.022	16 14 59.3	–27 50 22	−1.7 ± 0.1	0.3	4
GSC 06793-01406	SC	−0.6 ± 0.2	0.36 ± 0.01	G7	8.102 ± 0.018	16 16 18.0	–23 39 47	−6.7 ± 0.2	0.8	13
GSC 06214-02384	SC	fi	0.41 ± 0.01	K0	8.509 ± 0.019	16 19 34.0	–22 28 29	−3.5 ± 0.1	0.1	3
GSC 06794-00156	SC	−0.3 ± 0.1	0.34 ± 0.01	G6	7.084 ± 0.018	16 24 51.4	–22 39 32	−3.7 ± 0.7	1.3	4
GSC 06794-00537	SC	fi	0.48 ± 0.02	K2	8.184 ± 0.024	16 23 07.8	–23 00 59	−6.5 ± 0.6	1.0	3
GSC 06798-00035	SC	fi	0.35 ± 0.02	G1	7.695 ± 0.023	16 23 32.3	–25 23 48	−7.1 ± 0.3	0.2	2
GSC 06794-00337	SC	fi	0.44 ± 0.01	K1	8.084 ± 0.026	16 27 39.6	–22 45 22	−6.1 ± 0.1	0.1	4

[1] em = emission, abs = absorption fi = filled in; [2] GW Lup, EX Lup, HK Lup: also observed by Melo et al. (2003) and found to be single; [3] MN Lup: large v sin i possibly a spectroscopic binary but data insufficient; [4] HIP75836: listed in Simbad as eclipsing binary but no RV-variations observed, unlikely to be member of Lup; [5] GSC 06781-01046: this object might be a short-period SB2; [6] HBC 603 (Sz77): binary with separation of 1.″8 ± 0.″1 (Ghez et al. 1997); [7] GSC 06793-00569: asymmetric cross-correlation function, could be a visual binary.

Table 20. The single stars: ρ Ophiuchi, Corona Australis.

	Region	EW Hα[1] [Å]	EW LiI [Å]	spec type	m_K [mag]	RA (2000.0)	Dec (2000.0)	RV [km s^{-1}]	σ RV [km s^{-1}]	No. of spectra
RXJ1612.3-1909	Oph	−3.9 ± 0.1	≤1.0	M2.5	9.605 ± 0.019	16 12 20.9	–19 09 04	−1.6 ± 1.6	2.2	2
V1002 Sco	Oph	fi	0.48 ± 0.05	K0	7.494 ± 0.026	16 12 40.5	–18 59 28	−3.7 ± 1.0	1.4	2
V2503 Oph[2,3]	Oph	−57 ± 1	0.50 ± 0.03	K6-7	7.509 ± 0.031	16 25 10.5	–23 19 14	−7.1 ± 0.4	0.6	2
RXJ1625.3-2402	Oph	f1	0.52 ± 0.12	K5	8.764 ± 0.025	16 25 22.4	–24 02 06	−4.8 ± 0.3	0.4	2
V2058 Oph	Oph	−91 ± 12	0.45 ± 0.04	K5	7.518 ± 0.024	16 25 56.2	–24 20 48	−4.9 ± 0.3	0.7	3
V2129 Oph[2,4]	Oph	−22 ± 4	0.53 ± 0.02	K3.5	7.207 ± 0.023	16 27 40.3	–24 22 03	−6.8 ± 0.6	1.7	8
HBC 268 [2]	Oph	−42 ± 2	0.44 ± 0.02	K2-3	7.610 ± 0.024	16 31 33.5	–24 27 37	−6.3 ± 0.5	0.9	4
HD173148[5]	CrA	abs	0.27 ± 0.03	G5	7.204 ± 0.020	18 45 34.8	–37 50 20	0.1 ± 0.4	1.6	17
S CrA [2,6]	CrA	−51 ± 6	0.20 ± 0.01	K6	6.107 ± 0.021	19 01 08.6	–36 57 20	0.9 ± 0.9	1.6	3
V709 CrA	CrA	fi	0.40 ± 0.02	K0	7.713 ± 0.021	19 01 34.9	–37 00 57	−1.3 ± 0.3	0.7	6
DG CrA	CrA	−53 ± 16	0.36 ± 0.03		7.952 ± 0.026	19 01 55.2	–37 23 41	−1.8 ± 0.4	0.9	6
V702 CrA	CrA	abs,fi	0.32 ± 0.01	G5	8.354 ± 0.027	19 02 02.0	–37 07 44	−0.7 ± 0.1	0.5	19
HBC 679	CrA	fi	0.48 ± 0.03	K5	9.229 ± 0.030	19 02 22.1	–36 55 41	−0.1 ± 0.3	0.5	3
Kn Hα14[7]	CrA	−27 ± 13	0.53 ± 0.08	M0	8.446 ± 0.017	19 02 33.1	–36 58 21	10.5 ± 4.4	12	9

[1] em = emission, abs = absorption fi = filled in; [2] V2503 Oph (Haro 1-4), V2129 Oph (SR 9), HBC 268 (Haro 1-16), S CrA also observed by Melo et al. (2003) and found to be single; [3] V2503 Oph (Haro 1-4): binary with separation of 0.″72 (Ghez et al. 1997); [4] V2129 Oph (SR 9): binary with separation of 0.″59 (Ghez et al. 1997); [5] HD173148: binary with separation of 1.″1; [6] S CrA: binary with separation of 1.″41 ± 0.″06 (Ghez et al. 1997); [7] Kn Hα14: this might be a spectroscopic binary.